Molecular Crystals and Liquid Crystals

ISSN: 1542-1406 (Print) 1563-5287 (Online) Journal homepage: http://www.tandfonline.com/loi/gmcl20

Bifurcated-tail chiral fluorinated organosiloxane liquid crystalline materials

W. Michael Zoghaib, Carlo Carboni, Jokha Al-Rawahi, Fatma Al-Rubaiei, Haitham Al-Bulushi, Maryam Al-Aufi, Marwa Al-Harrasi, Shirin Al-Kalbani & Abir Al-Kiyumi

To cite this article: W. Michael Zoghaib, Carlo Carboni, Jokha Al-Rawahi, Fatma Al-Rubaiei, Haitham Al-Bulushi, Maryam Al-Aufi, Marwa Al-Harrasi, Shirin Al-Kalbani & Abir Al-Kiyumi (2016) Bifurcated-tail chiral fluorinated organosiloxane liquid crystalline materials, Molecular Crystals and Liquid Crystals, 632:1, 114-123

To link to this article: http://dx.doi.org/10.1080/15421406.2016.1185592

Published online: 17 Aug 2016.

MOLECULAR CRYSTALS AND LIQUID CRYSTALS
2016, VOL. 632, 114–123
http://dx.doi.org/10.1080/15421406.2016.1185592

Taylor & Francis
Taylor & Francis Group

Bifurcated-tail chiral fluorinated organosiloxane liquid crystalline materials

W. Michael Zoghaib[a], Carlo Carboni[b], Jokha Al-Rawahi[a], Fatma Al-Rubaiei[a], Haitham Al-Bulushi[a], Maryam Al-Aufi[a], Marwa Al-Harrasi[a], Shirin Al-Kalbani[a], and Abir Al-Kiyumi[a]

[a]Chemistry Department, Sultan Qaboos University, Al-Khod, Oman; [b]Physics Department, Sultan Qaboos University, Al-Khod, Oman

ABSTRACT
The synthesis and characterization of a series of chiral fluorinated low molar mass (bifurcated tail) organosiloxane materials is presented. The mesogenic moiety is similar to that in the TSiKN65F mesogen reported by Naciri et al., which displays a de Vries-type S_A^* phase. The one parameter varied across the series reported herein is the length of the alkyl chain linking the mesogen moiety to the bifurcated siloxane tail.

KEYWORDS
de-Vries phase; organosiloxane; bifurcated siloxane tail; chiral; smectic

1. Introduction

Ferroelectric liquid crystalline materials are of great interest due to their important industrial applications. Low molar mass organosiloxane liquid crystals are good candidates for the search of materials displaying de-Vries type phases [1–5] and have demonstrated fast switching in the S_A [6] and S_C* phases [7–9]. Ferroelectricity is exhibited in liquid crystal molecules if the molecules are chiral (no plane of symmetry), have a dipole moment directed perpendicular to the molecular axis and if molecules are tilted with respect to the smectic layer normal. Liquid crystalline materials exhibiting chiral smectic C phase below room temperature are of great importance due to their use in flat-panel displays and light modulators [10–14].

The materials we are reporting in this communication consist of a rigid core connected to a long chain hydrocarbon head and ending with a bifurcated trisiloxane terminus. Using three phenyl rings as the mesogenic core unit, potentially produces a wider liquid crystalline phase temperature range. The introduction of a siloxane terminus reduces the phase transition temperature, broadens the liquid crystal temperature range, helps the smectic phase formation and stabilization and enhances the molecule's spontaneous polarization [15–17].

Many lateral substituents have been introduced to the mesogenic core of liquid crystal materials, the most common is a fluorine substituent. The small size of a fluorine substituent enables its incorporation into all types of liquid crystals including, calamitic, discotic and lyotropic. However, fluorine with its high electronegativity leads to significant modification of liquid crystalline physical properties without too much disruption to the LC phase stability. The fluoro substituent modifies melting point, mesophase morphology and transition

CONTACT W. Michael Zoghaib zoghaibw@squ.edu.om Chemistry Department, Sultan Qaboos University, PO Box 36, Al-Khod 123, Oman.
Color versions of one or more of the figures in the article can be found online at www.tandfonline.com/gmcl.

temperature. It also decreases the melting point and T_{N-1} (the upper temperature limit) of the LC phase. Increasing the number of substituents further decreases the T_{N-1} but only slightly decreases the melting point [18]. Varying the hydrocarbon chain length modifies the macroscopic properties of mesogenic materials. It is well documented that rotational viscosities and tilt angles of chiral smectic C (S_C^*) molecules increase with increasing chain length [19].

2. Experimental

2.1 Materials

Reagents were purchased from Aldrich and used as received. The catalyst dichlorodicyclopentadienyl platinum II was purchased from STREM Chemicals (Massachusetts, USA) and 1, 1, 1, 3, 5, 5, 5-heptamethyltrisiloxane was purchased from CHEM HERE (Hong Kong).

2.2 Methods

Proton Magnetic Resonance (^{1}H-NMR) spectra were acquired and recorded using either a 400 MHz VARIAN NMR spectrometer or a 700 MHz BRUKER NMR spectrometer (indicated with each compound) in $CDCl_3$. Carbon Magnetic Resonance (^{13}C-NMR) spectra were recorded for each compound using the same NMR spectrometer for ^{1}H acquisition. Chemical shifts (δ_{ppm}) were recorded in parts per million (ppm) downfield from TMS (assigned as zero ppm).

Thin layer chromatography (TLC) and preparative TLC were performed on glass plates pre-coated with silica gel, whereas flash column chromatography was performed using silica gel 60 (mesh 70–230) purchased from Aldrich.

Rotary evaporator (BUCHI) was used to evaporate solvents at low pressure. Anhydrous reaction conditions were performed under an inert atmosphere of dry Argon. THF was dried by distillation over potassium metal under Argon and used immediately.

Liquid crystal transition temperatures were identified by polarized light microscopy in conjunction with a heating/cooling stage and a temperature control unit (Linkam TMS 94). The specimens were filled by capillary action at a temperature of about 20 degrees above the transition to isotropic phase into a 5 μm thick glass cell treated for planar alignment. An indium tin oxide (ITO) transparent electrode was soldered to the inner face of the glass cell facilitating the application of an electric field to the specimen.

The tilt angle is measured as half the angle between the two positions of extinction when the specimen is switched between crossed polarizers.

3. Synthesis

Preparation of compounds **1** to **6** from commercially available starting materials was described in earlier communications [4,5].

Synthesis of the homologous mesogenic series of compounds **7** to **12** (Figure 1) was performed according to the following general method.

To a stirred solution of each of **1, 2, 3, 4, 5 and 6** in anhydrous THF (5 mL) under argon, the silylating reagent 1, 1, 1, 3, 5, 5, 5-heptamethyltrisiloxane (*l*) (1.2 molar equivalents) was added to give a yellow solution. Dichlorodicyclopentadienyl platinum II(*s*) (1 or 2 mg, 0.025 to 0.50 mmol) was added to the mixture and the solution's color turned black after gas evolution was noticed. The reaction was monitored by TLC and quenched by adding methanol when

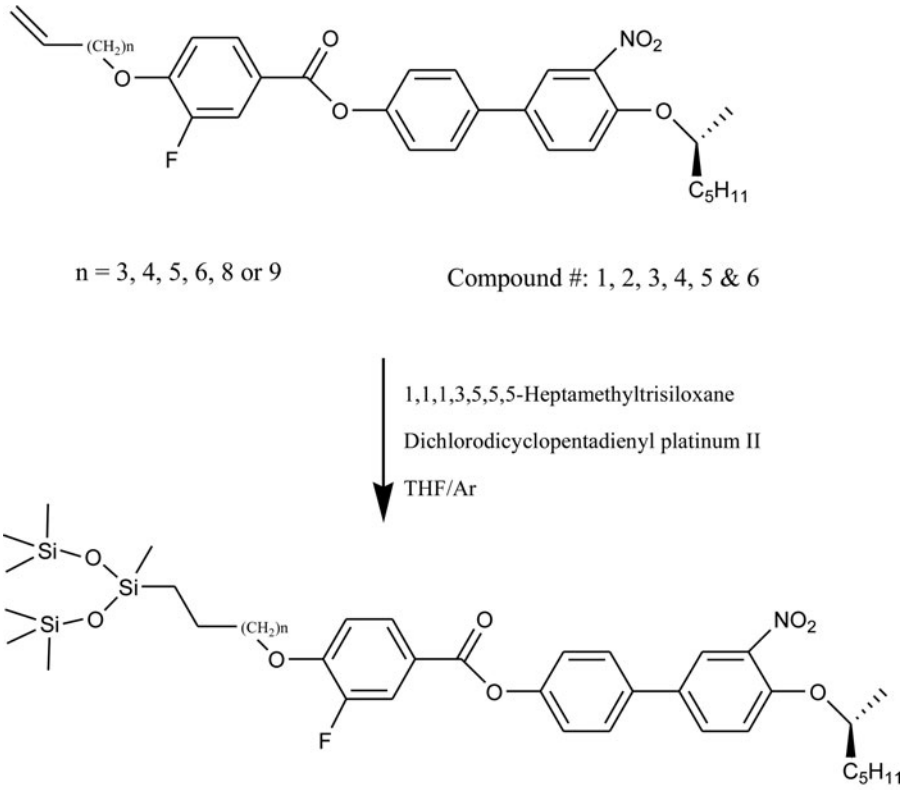

Figure 1. Preparation of bifurcated tail liquid crystals 7 – 12 from their precursors.

all starting material disappeared after an average of 90 minutes. The crude was purified by flash column chromatography on silica gel (eluent: 10% ethyl acetate/hexane) followed by preparative TLC using the same solvent system to yield a pure product.

(R)-4'-(heptan-2-yloxy)-3'-nitro-[1,1'-biphenyl]-4-yl-3-fluoro-4-((5-(1, 1, 1, 3, 5, 5, 5-heptamethyltrisiloxanyl)pentyl)oxy)benzoate (7)

(84.6% yield)

^{1}H NMR (BRUKER 700 MHz, $CDCl_3$) δ (ppm): 0.12 (m, 21H, CH_3 (32, 33, 33', 33",34, 34', 34"), 0.93 (t, 3H, CH_3(1), J 7.1 Hz), 1.14–1.30 (m, 12H, CH_2 (2, 3, 4, 29, 30, 31), 1.41 (d, 3H, CH_3(7), J 6.0 Hz), 1.55–1.61 (m, 2H, CH_2(5)), 1.77–1.84 (m, 2H, CH_2(28)), 4.07 (t, 2H, CH_2(27), J 6.6 Hz), 4.48 (sextet, 1H, CH(6), J 6.4 Hz), 7.06 (t, 1H, ArH (25), J 8.3 Hz), 7.16 (d, 1H ArH (09), J 8.6 Hz) 7.31 (d, 2H, ArH (15,16), J 8.6 Hz), 7.65 (d, 2H, ArH (17,18), J 8.6 Hz), 7.72 (dd, 1H, ArH (22) J 2.4, 8.7 Hz), 7.94 (dd, 1H, ArH (12), J 2.1, 11.4 Hz), 8.01 (dd, 1H, ArH (11), J 1.2, 8.6 Hz), 8.02 (d, 1H, ArH (23), J 8.5 Hz), 7.92 (d, 1H, ArH (12), J 2.3 Hz).

^{13}C NMR (BRUKER 176 MHz, $CDCl_3$) δ (ppm): 4.2 CH_3 (34, 34', 34"), 5.9 CH_3 (33, 33',33"), 2.8 CH_3 (32), 21.3 CH_2 (31), 33.5 CH_2 (30), 26.3 CH_2 (29), 30.6 CH_2 (28), 68.9 CH_2 (27), 151.0 C (26), 115.7 CH (25), 152.1 C (24), 126.3 CH (23), 117.7 CH (22), 123.8 C (21), 164.0 C (20), 152.0 C (19), 121.9 CH (18,17), 127.8 CH (16,15), 133.4 C (14), 129.1 C (13),

123.1 CH (12), 134.1 CH (11), 134.6 C (10), 115.6 CH (9), 152.8 C (8), 22.0 CH_3 (7), 70.1 CH (6), 32.8 CH_2 (5), 23.8 CH_2 (4), 23.2 CH_2 (3), 23.0 CH_2 (2), 20.4 CH_3 (1).

(R)-4′-(heptan-2-yloxy)-3′-nitro-[1,1′-biphenyl]-4-yl-3-fluoro-4-((6-(1, 1, 1, 3, 5, 5, 5-heptamethyltrisiloxanyl)hexyl)oxy)benzoate (8)

(75.0% yield)

^{1}H NMR (BRUKER 700 MHz, $CDCl_3$) δ (ppm): −0.02–0.08 (m, 21H, CH_3 (33, 34, 34',34",35, 35', 35"), 0.67–0.87 (m, 3H, CH_3(1)), 1.14–1.30 (m, 14H, CH_2 (2, 3, 4, 29, 30, 31, 32), 1.32 (d, 3H, CH_3 (7), J 6.0 Hz), 1.55–1.61 (m, 2H, CH_2 (5)), 1.77–1.84 (m, 2H, CH_2(28)), 4.06 (t, 2H, CH_2 (27), J 6.6 Hz), 4.47 (sextet, 1H, CH(6) J 6.3 Hz), 7.02 (t, 1H, ArH (25), J 8.4 Hz), 7.11 (d, 1H, ArH (9), J 9.0 Hz), 7.27 (d, 2H, ArH (17, 18), J 8.6 Hz), 7.57 (d, 2H, ArH (15, 16), J 8.6 Hz), 7.67 (dd, 1H, ArH (11), J 2.4, 8.4 Hz), 7.88 (dd, 1H, ArH (22) J 2.0, 11.5 Hz), 7.95 (d, 1H, ArH (23), J 8.5 Hz), 7.98 (d, 1H, ArH (12), J 2.3 Hz).

^{13}C NMR (BRUKER 176 MHz, $CDCl_3$) δ (ppm): 4.2 CH_3 (35, 35', 35"), 5.9 CH_3 (34, 34',34"), 2.0 CH_3 (33), 17.9 CH_2 (32), 21.3 CH_2 (31), 33.5 CH_2 (30), 26.3 CH_2 (29), 30.6 CH_2 (28), 69.5 CH_2 (27), 151.0 C (26), 115.7 CH (25), 147.7 C (24), 126.3 CH (23), 117.7 CH (22), 123.8 C (21), 164.1 C (20), 152.0 C (19), 121.9 CH (18,17), 127.8 CH (16,15), 133.4 C (14), 129.1 C (13), 123.1 CH (12), 134.1 CH (11), 134.6 C (10), 115.6 CH (9), 152.5 C (8), 22.4 CH_3 (7), 70.3 CH (6), 32.8 CH_2 (5), 23.8 CH_2 (4), 23.4 CH_2 (3), 23.1 CH_2 (2), 20.2 CH_3 (1).

(R)-4′-(heptan-2-yloxy)-3′-nitro-[1,1′-biphenyl]-4-yl-3-fluoro-4-((7-(1, 1, 1, 3, 5, 5, 5-heptamethyltrisiloxanyl)heptyl)oxy)benzoate (9)

(82.8% yield)

^{1}H NMR (BRUKER 700 MHz, $CDCl_3$) δ (ppm): −0.018–0.09 (m, 21H, CH_3 (34, 35, 35', 35", 36, 36', 36"), 0.79–0.84 (m, 3H, CH_3 (1)), 1.21–1.84 (m, 16H, CH_2 (2, 3,4, 29, 30, 31, 32, 33), 1.32 (d, 3H, CH_3(7), J 6.0 Hz), 1.55–1.61 (m, 2H, CH_2 (5)), 1.77–1.84 (m, 2H, CH_2 (28)), 4.06 (t, 2H, CH_2 (27), J 6.6 Hz), 4.48 (sextet, 1H, CH(6) J 6.4 Hz), 6.97 (t, 1H, ArH (25), J 8.4 Hz), 7.21 (d, 2H, ArH (17, 18), J 8.6 Hz), 7.51 (d, 2H, ArH (15, 16), J 8.6 Hz), 7.83 (dd, 1H, ArH (22) J 2.0, 11.5 Hz), 7.62 (dd, 1H, ArH (11), J 2.4, 8.4 Hz), 7.91 (d, 1H, ArH (09), J 8.4 Hz), 7.90 (d, 1H, ArH (23), J 8.5 Hz), 7.92 (d, 1H, ArH (12), J 2.3 Hz).

^{13}C NMR (BRUKER 176 MHz, $CDCl_3$) δ (ppm): 5.0 CH_3 (36, 36', 36"), 3.4 CH_3 (35, 35"), 2.8 CH_3 (34, 34'), 16.5 CH_2 (33), 17.9 CH_2 (32), 21.3 CH_2 (31), 33.5 CH_2 (30), 26.3 CH_2 (29), 30.6 CH_2 (28), 72.3 CH_2 (27), 151.0 C (26), 115.7 CH (25), 147.7 C (24), 126.3 CH (23), 117.7 CH (22), 123.8 C (21), 164.0 C (20), 152.0 C (19), 121.9 CH (18,17), 127.8 CH (16,15), 133.4 C (14), 129.1 C (13), 123.1 CH (12), 134.1 CH (11), 134.6 C (10), 115.6 CH (9), 152.5 C (8), 23.0 CH_3 (7), 70.1 CH (6), 32.8 CH_2 (5), 23.8 CH_2 (4), 22.5 CH_2 (3), 22.0 CH_2 (2), 15.4 CH_3 (1).

(R)-4′-(heptan-2-yloxy)-3′-nitro-[1,1′-biphenyl]-4-yl-3-fluoro-4-((8-(1, 1, 1, 3, 5, 5, 5-heptamethyltrisiloxanyl)octyl)oxy)benzoate (10)

(69.2% yield)

^{1}H NMR (BRUKER 400 MHz, $CDCl_3$) δ (ppm): − 0.015–0.10 (m, 21H, CH_3 (35, 36, 36', 36", 37, 37', 37"), 0.80–0.88 (m, 3H, CH_3(1)), 1.10–1.61 (m, 18H, CH_2 (2, 3, 4, 29, 30, 31, 32, 33, 34), 1.30 (d, 3H, CH_3(7), J 6.0 Hz), 1.55–1.61 (m, 2H, CH_2(5)), 1.70–1.82 (m, 2H, CH_2(28)), 4.08 (t, 2H, CH_2(27), J 6.6 Hz), 4.35 (sextet, 1H, CH(6) J 6.4 Hz), 6.97 (t, 1H, ArH(25), J 8.4 Hz),

7.21(d, 2H, ArH(17,18), J 8.6 Hz), 7.51 (d, 2H, ArH(15,16), J 8.6 Hz), 7.83 (dd, 1H, ArH(22) J 2.0, 11.5 Hz), 7.60 (dd, 1H, ArH(11), J 2.4, 8.4 Hz), 7.85 (d, 1H, ArH(09), J 8.4 Hz), 7.90 (d, 1H, ArH(23), J 8.5 Hz), 7.92 (d, 1H, ArH(12), J 2.3 Hz).

^{13}C NMR (BRUKER 100 MHz, $CDCl_3$) δ (ppm): 4.2 CH_3 (37, 37', 37"), 5.5 CH_3 (36, 36', 36"), 2.1 CH_3 (35), 16.0 CH_2 (34), 16.5 CH_2 (33), 17.9 CH_2 (32), 21.5 CH_2 (31), 33.4 CH_2 (30), 26.5 CH_2 (29), 30.4 CH_2 (28), 72.3 CH_2 (27), 151.0 C (26), 115.7 CH (25), 147.8 C (24), 126.3 CH (23), 117.6 CH (22), 123.8 C (21), 164.0 C (20), 152.0 C (19), 121.9 CH (18, 17), 127.8 CH (16, 15), 133.4 C (14), 129.1 C (13), 123.1 CH (12), 134.1 CH (11), 134.6 C (10), 115.6 CH (9), 152.2 C (8), 24.1 CH_3 (7), 70.3 CH (6), 32.8 CH_2 (5), 23.7 CH_2 (4), 21.5 CH_2 (3), 20.0 CH_2 (2), 14.4 CH_3 (1).

(R)-4'-(heptan-2-yloxy)-3'-nitro-[1,1'-biphenyl]-4-yl-3-fluoro-4-((10-(1, 1, 1, 3, 5, 5, 5-heptamethyltrisiloxanyl)decyl)oxy)benzoate (11)

(63.0% yield)

^{1}H NMR (BRUKER 400 MHz, $CDCl_3$) δ (ppm): 0.059–0.090 (m, 18H, CH_3(38, 38', 38", 39, 39', 39")), 0.12 (s, 3H CH_3 (37)), 0.88–0.91 (t, 3H, CH_3 (1), 1.26–1.34 (m, 22H, CH_2 (2, 3, 4, 29, 30, 31, 32, 33, 34, 35, 36), 1.35 (d, 3H, CH_3(7) J 6.0 Hz), 1.50 (m, 2H, CH_2(5)), 1.87–1.95 (m, 2H, CH_2(28)), 4.11 (t, 2H, CH_2(27) J 6.6 Hz), 4.45–4.51 (sextet, 1H, CH(6) J 6.4 Hz), 6.97 (t, 1H, ArH(25) J 8.3 Hz), 7.13 (d, 1H, ArH(9) J 8.4 Hz), 7.21 (t, 2H, ArH(17,18) J 8.6 Hz), 7.55 (d, 2H, ArH(15,16) J 8.6 Hz), 7.65 (dd, 2H, ArH(22) J 2.0, 11.5 Hz), 7.86 (dd, 2H, ArH (11) J 2.4, 8.4 Hz), 7.92 (d, 1H, ArH(23) J 8.5 Hz), 7.94 (d, 1H, ArH(12) J 2.3 Hz).

^{13}C NMR (BRUKER 100 MHz, $CDCl_3$) δ (ppm): 0.13 CH_3 (37, 37'), 0.49 CH_3 (39, 39', 39'), 0.80 CH_3 (38, 38'), 13.1 CH_3(1), 18.0 CH_2(36), 19.4 CH_2(35), 22.4 CH_3(7), 23.0 CH_2(2), 24.8 CH_2(4), 25.8 CH_2(29), 26.3 CH_2(28), 28.8 CH_2(30), 29.2 CH_2(31), 29.4 CH_2(32), 31.5 CH_2(3), 33.2 CH_2(34), 39.9 CH_2(5), 69.3 CH_2(27), 70.4 CH (6), 113.2 ArCH (22), 116.5 ArCH (9), 118.2 ArCH (25), 122.1 ArCH (17,18), 123.6 ArCH (12), 127.3 C(21), 127.6 ArCH (15,16), 131.8 ArC (13), 132.3 ArC (14), 136.2 ArC (10), 136.6 ArCH (11), 140.8 ArC (19), 150.4 ArC (26), 151.82 ArC (24), 153.4 ArCH (8), 163.9 C=O (20).

(R)-4'-(heptan-2-yloxy)-3'-nitro-[1,1'-biphenyl]-4-yl-3-fluoro-4-((11-(1, 1, 1, 3, 5, 5, 5-heptamethyltrisiloxanyl)undecyl)oxy)benzoate (12)

(51.5% yield)

^{1}H NMR (400 MHz, $CDCl_3$) δ (ppm): 0.020–0.080 (m, 21H, CH_3 (38, 39, 39', 39", 40, 40', 40")), 0.81 (m, 2H, CH_2 (37), 1.18–1.29 (m, 18H, CH_2 (2,3, 4, 29, 30, 31, 32, 33, 34)), 1.33 (d, 3H, CH_3(7) J 6.0 Hz), 1.36–1.46 (m, 4H,CH_2 (34,35), 1.53 (m, 2H, CH_2(5)), 1.78–1.83 (m, 2H, CH_2(28)), 4.13 (t, 2H, CH_2 (27) J 6.6 Hz), 4.50–4.60 (m, 1H, CH(6)), 7.05 (t, 1H, ArH(25) J 8.0 Hz), 7.14 (d, 1H, ArH(9) J 8.4 Hz), 7.29 (d, 2H, ArH (17,18) J 8.6 Hz), 7.59 (d, 2H, ArH (15,16) J 8.6 Hz), 7.71 (dd, 2H, ArH(22) J 2.0, 11.5 Hz), 7.86 (dd, 2H, ArH(11) J 2.4, 8.4 Hz), 7.90 (d, 1H, ArH(23) J 8.5 Hz), 7.93 (d, 1H, ArH(12) J 2.3 Hz).

^{13}C NMR (100 MHz, $CDCl_3$) δ (ppm): 1.3 CH_3 (38), 13.0 CH_3 (39, 39', 39"), 13.1 CH_3 (40, 40', 40"), 14.1 CH_3 (1), 17.9 CH_2 (37), 18.1 CH_2 (36), 19.4 CH_2 (35), 22.4 CH_3 (7), 23.0 CH_2 (2), 24.8 CH_2 (4), 25.1 CH_2 (29), 25.4 CH_2 (28), 27.9 CH_2 (30), 28.2 CH_2 (31), 28.4 CH_2 (32), 28.5 CH_2 (3), 30.8 CH_2 (34), 35.3 CH_2 (5), 68.1 CH_2 (27), 68.4 CH (6), 112.4 ArCH (22), 115.1 ArCH (9), 116.9 ArCH (25), 121.3 ArCH (17,18), 122.8 ArCH (12), 126.4 C (21), 126.7 ArCH (15, 16), 131.8 ArC (13), 130.9 ArC (14), 131.4 ArC (10), 135.3 ArCH (11), 140.0 ArC (19), 150.9 ArC (26), 151.1 ArC (24), 152.1 ArCH (8), 163.1 C=O (20).

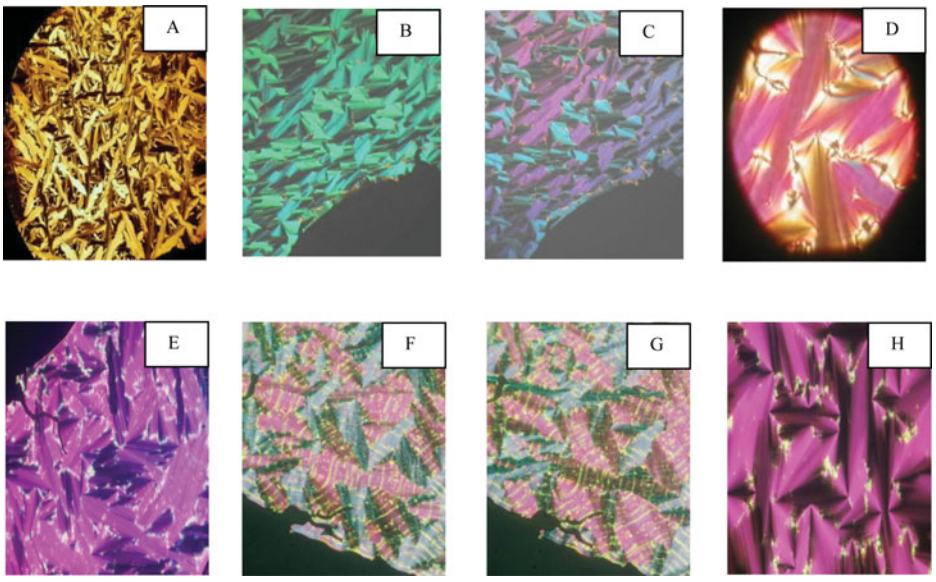

Plate 1. Some of the textures observed in the aforementioned series of materials (LC # 7 to LC # 12). **A**: LC 7 at 49°C. **B**: LC # 8 at −10°C, field of +9 V/μm applied. **C**: LC # 8 at −10°C, field of −9 V/μm applied. **D**: LC # 9 at 24°C with no field applied. **E**: LC # 10 at 50°C with no field applied. **F**: LC # 11 at −18°C, field of +12 V/μm applied. **G**: LC # 11 at −18°C, field of -12 V/μm applied. **H**: LC # 12 at 75°C.

4. Polarized light microscopy observations

The observations are summarized in Table 1 and texture observations are displayed in Plate 1. As it is usually the case with low molar mass organosiloxane materials there is a direct transition between the isotropic and smectic phases. The transition occurs through a 4 to 5 degree biphasic range. In almost all specimens upon cooling, small bâtonnets appear in the isotropic phase, the bâtonnets do not grow in size but their number increases to give the sanded texture often observed in organosiloxane materials.

On cooling LC # 12, the specimen displays a direct transition to a smectic phase. The domains growing display a focal conic texture which is typical of a smectic phase. The domains multiply and grow until the whole specimen is in the smectic phase. At temperatures just below the transition the specimen shows some response to an electric field but the response is not that of a ferro-electric S_C^* phase. Dark domains remain dark when the field is reversed.

Table 1. Transition temperatures of liquid crystals **7** – **12**.

LC # 7	K $\underset{-16^\circ C}{\longleftrightarrow}$ S_A^* $\underset{49^\circ C}{\longleftrightarrow}$ I
LC # 8	K $\underset{-21^\circ C}{\longleftrightarrow}$ S_C^* $\underset{17^\circ C}{\longleftrightarrow}$ S_A^* $\underset{47^\circ C}{\longleftrightarrow}$ I
LC # 9	K $\underset{-18^\circ C}{\longleftrightarrow}$ S_C^* $\underset{20^\circ C}{\longleftrightarrow}$ S_A^* $\underset{57^\circ C}{\longleftrightarrow}$ I
LC # 10	Cr $\underset{-20^\circ C}{\longleftrightarrow}$ S_C^* $\underset{55^\circ C}{\longleftrightarrow}$ I
LC # 11	Cr $\underset{-26^\circ C}{\longleftrightarrow}$ S_C^* $\underset{90^\circ C}{\longleftrightarrow}$ I
LC # 12	K $\underset{-22^\circ C}{\longleftrightarrow}$ S_C^* $\underset{53^\circ C}{\longleftrightarrow}$ S_A^* $\underset{83^\circ C}{\longleftrightarrow}$ I

Sc*: Chiral smectic C S_A*: chiral smectic A K: Glass phase Cr: Crystalline phase I: isotropic

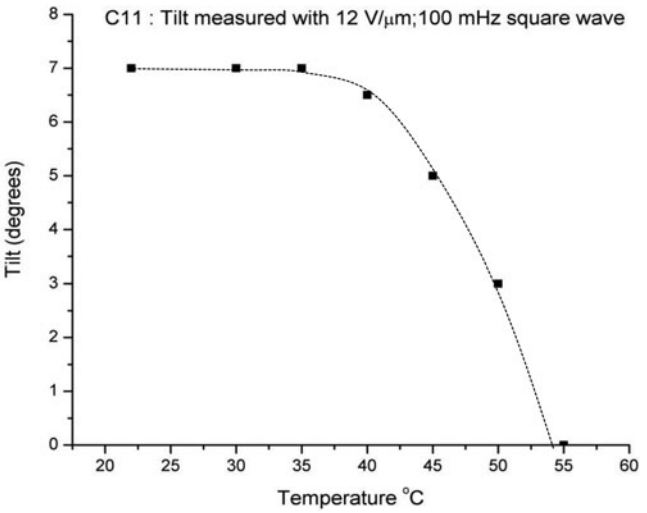

Figure 2. Tilt angle measurement in LC # 12.

This observation indicates that the phase is a smectic A phase. At lower temperatures the switching in the electric field becomes characteristic of a smectic C* phase. The tilt angle in LC # 12 goes to zero degrees at about 54 °C (Figure 2).

On cooling LC # 11 from the isotropic phase, the specimen displays a direct transition to the smectic phase. Domains displaying focal conic texture appear with their layers perpendicular to the glass surface. The domains multiply and grow until the whole specimen is in the smectic phase. The specimen responds to an electric field whereby dark domains can be switched to bright when the electric field is reversed. This indicates that the phase is a smectic C* phase. The molecules are tilted to one side of the layer normal when the field is up and tilted to the other side when the field is down. By rotating the specimen between the two dark states the tilt angle θ can be measured. The tilt angle in this specimen is about 10 degrees and is almost independent of temperature and of applied field magnitude. This is in agreement with what has been reported on other organosiloxane materials displaying a smectic C phase [20].

On cooling LC # 9, the specimen displays the sanded texture with small focal conics observed in most organosiloxane materials.

The application of a square wave electric field of 8 V/μm causes the specimen to align in some larger domain. A uniform alignment of the specimen was not achieved. At room temperature the material appears to be in the smectic A phase, on cooling below room temperature ferroelectric switching is observed indicating that there is a transition to the smectic C phase. At 13°C the tilt angle is about 9 degrees. The response time for switching with a field of 12 V/μm at this temperature is 100 μs. The response time increases as the temperature is decreased and switching ceases to be observable at −18°C.

In LC # 8, the tilt shows a strong dependence on the applied field amplitude; This would suggest that the S_C^* phase is a de Vries type S_C^*. The saturation field appears to be quite high so that at 0°C there is no sign of saturation even at the highest field applied. At −10°C there is a beginning of saturation at about 9 V/μm; by extrapolation one could infer that the molecular tilt is around 20 degrees.Figure 3 shows the relationship between applied field and tilt angle.

An electro-clinic coefficient can be derived from the linear portion of the graph (Table 2):

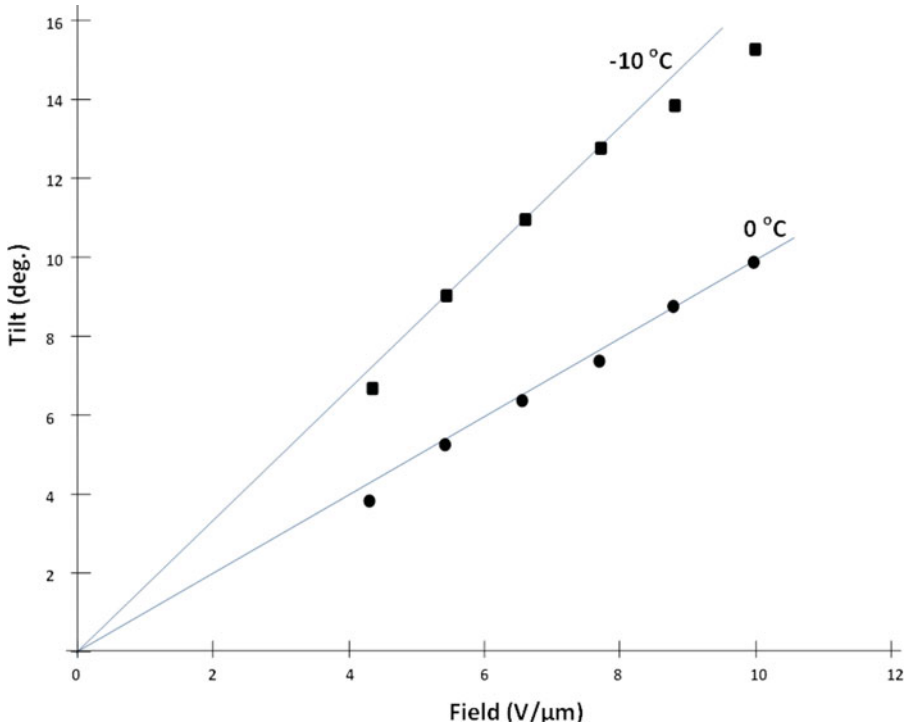

Figure 3. Tilt angle dependence on applied field magnitude in LC # 8.

Table 2. Temperature and corresponding electro-clinic coefficient for LC # 8.

Temperature (°C)	Electro-clinic coefficient. (Degree/Vμm^{-1})
0	1.0
−10	5.8

In LC # 7, the measurements were taken as a function of the field applied amplitude at selected fixed temperatures. The response observed is that of a $S_A{}^*$ phase with a large electro-clinic effect. The induced tilt angle increases linearly with the field amplitude. The fact that no sign of saturation was observed even at the large 24 V/μm field would suggest that the phase is not a de Vries type phase as observed in several other low molar mass organosiloxane materials however, the large electro-clinic response and the temperature behavior would suggest otherwise (Table 3 and Figure 4).

Plate 1 displays some of the textures observed during phase transition measurements.

Table 3. Temperature and corresponding electro-clinic coefficient for LC # 7.

Temperature (°C)	Electro-clinic coefficient (Degree/Vμm^{-1})
−10	2.68
0	2.21
+10	1.62

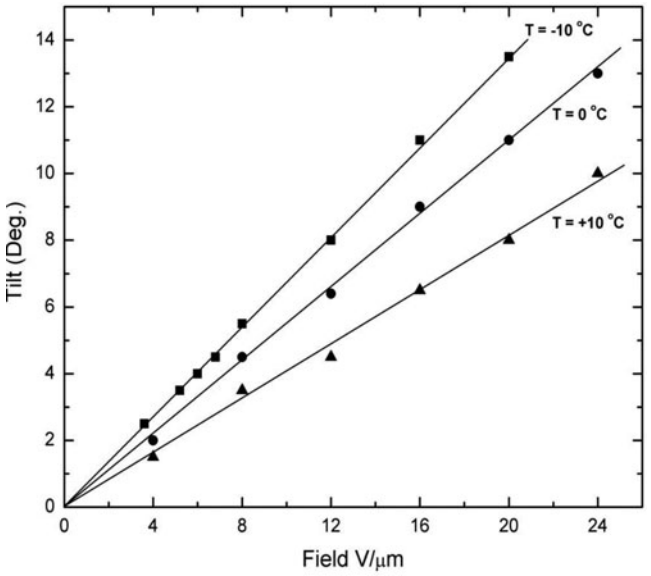

Figure 4. Tilt angle dependence on applied field magnitude in LC # 7.

5. Conclusion

A new series of six chiral fluorinated organosiloxane liquid crystals was prepared with a yield ranging from moderate to good. All six LCs (differing only in the length of the hydrocarbon chain connecting the rigid core to the bifurcated siloxane terminus) exhibit one or more smectic phases over a wide temperature range. LCs # 8, 9 and 12 exhibit both S_A^* and S_C^* phases upon cooling from the isotropic whereas LCs # 10 and 11 possess only a S_C^* phase. LC # 7 shows a de Vries type S_A^* phase. Where applicable, the tilt angle as a function of temperature or applied field magnitude was measured.

Acknowledgment

Financial support by Sultan Qaboos University's Internal Grant number IG/SI/PHYS/12/03 is greatly appreciated.

References

[1] Kanbe, J., Inoue, H., Mizutome, A., Hanyuu, Y., Katagiri, K., & Yoshihara, S. (1991) *Ferroelectrics*, *114*, 3.
[2] Sprunt, S., Naciri, J., Ratna, B. R., & Shashidar, R. (1995). *Appl. Phys. Lett.*, *66*, 1443.
[3] Handaschy, M. A., Drabik, T. J., Cotter, L. K., & Gaalema, S. D. (1990). *Optical Digital GaAs Technology, Signal processing Applications; Proc. SPIE*, *1291*, 158.
[4] Naciri, J., Ruth, J., Crawford, G., Shashindar, R., & Ratna, B. R. (1995). *Chem. Mater*, *7*, 1397.
[5] Zoghaib, W. M., Carboni, C., George, A. K., AL-Manthari, S., AL-Hussaini, A., & AL-Futaisi, F. (2011). *Mol. Cryst. Liq. Cryst.*, *542*, 123.
[6] Newton, J., Coles, H. J., Hodge, P., & Hannington, J. (1994). *J. Mater. Chem.*, *4*, 869–874.
[7] Coles, H. J., Owen, H., Newton, J., & Hodge, P. (1993). *Liq. Cryst.*, *15*, 739–744.
[8] Coles, H. J., Owen, H., Newton, J., & Hodge, P. (1995). *Proc. SPIE*, *2408*, 22–29.
[9] Kloess, P., McComb, J., Coles, H. J., & Zentel, R. (1996). *Ferroelectrics*, *180*, 233–243.
[10] Lagerwall, S. T., & Dahl, I. (1984). *Mol. Cryst. Liq. Cryst.*, *114*, 151–187.
[11] Lagerwall, S. T., Otterholm, B., & Skarp, K. (1987). *Mol. Cryst. Liq. Cryst.*, *152*, 503–587.

[12] Roberts, J. C., Kapernaum, N., Giesselmann, F., Wand, M. D., & Lemieux, R. P. (2008). *J. Mater. Chem.*, *18*, 5301–5306.
[13] Grüneberg, K., Naciri, J., & Shashidhar, R. (1996). *Chem. Mater.*, *8*, 2486–2498.
[14] Keith, C., Reddy, R. A., Baumeister, U., & Tschierske, C. (2004). *J. Am. Chem. Soc.*, *126*, 14312–14313.
[15] Hsu, C. S., & Her, B. S. (1996). *Macromol. Chem. Phys.*, *197*, 4105–4118.
[16] Liao, C. T., Wu, Z. L., Wu, N. C., Liu, J. Y., Jiang, M. H., Zou, S. F., & Lee, J. Y. (2010). *Mol. Cryst. Liq. Cryst.*, *533*, 3–15.
[17] Leadbetter, A. J., Forst, J. C., & Mazid, M. A. (1979). *J. Physique Lett.*, *40*, 325–329.
[18] Collings, P. J., et al. (1997). In: *Introduction to Liquid Crystals*; Gray, G. W., Goodby, J. W., & Fukuda, A. (Eds.), Chapter 3, Taylor & Francis: London.
[19] Lin, Chih-Hung (2013). *International Journal of Molecular Sciences*, *14*, 21306.
[20] Robinson, W. K., Caboni, C., Kloess, P., Perkins, S. P., & Coles, H. J. (1998). *Liquid Crystals*, *25*, 301–307.